Formation of forearc basins and their influence on subduction zone earthquakes

Christopher W. Fuller
Sean D. Willett
Department of Earth and Space Sciences, University of Washington, Seattle, Washington, USA
Mark T. Brandon
Department of Geology and Geophysics, Yale University, New Haven, Connecticut, USA

ABSTRACT

Recent observations of an association between forearc basins and slip during subduction thrust earthquakes suggest a link between processes controlling upper plate structure and seismic coupling on the subduction-zone thrust fault. We present a mechanism for the formation of these basins where sedimentation occurs on landward-dipping segments of the subduction wedge, which itself is actively growing through the accretion of material from the subducting plate. Our numerical simulations demonstrate that sedimentation stabilizes the underlying wedge, preventing internal deformation beneath the basin. Maximum slip during great-thrust earthquakes tends to occur where sedimentary basins stabilize the overlaying wedge. The lack of deformation in these stable regions increases the likelihood of thermal pressurization of the subduction thrust, allows the fault to load faster, and allows greater healing of the fault between rupture events. These effects link deformation of the subduction wedge to the seismic coupling of the subduction thrust.

Keywords: forearc basins, subduction zone, critical wedge, numerical modeling, subduction wedge, subduction thrust earthquakes.

INTRODUCTION

The largest and most destructive earthquakes occur on subduction-zone thrust faults, where oceanic plates are consumed by underthrusting beneath adjacent plate margins (Kanamori, 1986). The slip that occurs during earthquakes only accounts for part of the total convergence between the oceanic plate and overriding plate as evident from variations in the degree of seismic coupling, defined as the ratio of seismic slip to total slip (Scholz, 1989). Seismic coupling varies spatially along a typical subduction zone, and yet remains relatively steady over multiple earthquake cycles (Thatcher, 1990). Evidence supporting the existence of variations in seismic coupling includes the observation that earthquake slip tends to occur in a patchy pattern along these faults. The areas of greatest seismic slip, and hence the greatest seismic coupling, are referred to as asperities (Lay et al., 1982; Kanamori, 1986; Thatcher, 1990). For example, subduction-thrust earthquakes along the Nankai suduction zone off southwest Japan (Fig. 1) show this characteristic behavior with seismic slip varying both parallel and normal to the strike of the subduction zone. Ultimately, the total magnitude of a subduction earthquake depends on the amount of slip and the total area over which it occurs, pointing to the importance of determining the physical controls on the distribution of seismic asperities.

Many studies have focused on the stress state, rheology, or temperature of the subduction thrust as an explanation for the distribution of seismic coupling (e.g., Kanamori, 1971; Kelleher et al., 1974; Ruff and Kanamori, 1980; Tichelaar and Ruff, 1993; Hyndman et al., 1995). However, deformation of the upper plate is also thought to affect the size and distribution of earthquakes (McCaffrey, 1994). Two recent studies (Song and Simons, 2003; Wells et al., 2003) show that seismic asperities preferentially occur where the overriding plate is overlain by forearc basins (Fig. 1), which suggests that the configuration of the overriding plate exerts a strong influence on seismic behavior of the underlying subduction thrust.

In regions where sedimentary material from the oceanic plate is being actively accreted to the margin, the upper plate tends to deform into a wedge-shape profile that tapers to a point where the subduction thrust reaches the surface (Davis et al., 1983) (Fig. 1B). Forearc basins represent a significant departure from this simple geometric form, yet their formation is also a consequence of permanent deformation of the overriding plate in response to subduction and accretion. We consider here the mechanics and tectonic evolution of forearc basins within an actively accreting and deforming subduction wedge. Our analysis is based on numerical experiments using a coupled mechanical-thermal model (Willett and Pope, 2003; Willett, 1992) that has been modified to simulate the evolution of a subduction wedge in response to shear tractions and the accretion of a thin sedimentary layer from the subducting oceanic plate (Fig. 2A). A detailed description of the numerical model is given in the Data Repository.[1]

MODEL RESULTS

The long-term evolution (over millions of years) of a typical subduction wedge is illustrated for two cases: Model 1 shows the evolution for a case where topographic depressions receive no sediment (Fig. 2B; Fig. DR2 and Video DR1 [see footnote 1]), and Model 2 shows the evolution of a margin where topographic depressions are filled to capacity with sediment (i.e., ''fill to spill'') (Fig. 2C; Fig. DR3 and Video DR2). The results shown here have a convergence velocity v_c of 50 km/m.y. and an accretionary thickness h of 2.5 km (Fig. DR1), indicating an accretionary flux of 125 km^2/m.y. The accretionary flux determines the rate at which the model wedges grow. For example, the Cascadia margin has

[1]GSA Data Repository item 2006018, details for numerical model, Figures DR1–DR3, and videos of models 1 and 2, is available at www.geosociety.org/pubs/2006.htm, or on request from editing@geosociety.org or Documents Secretary, GSA, P.O. Box 9140, Boulder, CO 80301-9140.

© 2006 Geological Society of America. For permission to copy, contact Copyright Permissions, GSA, or editing@geosociety.org.

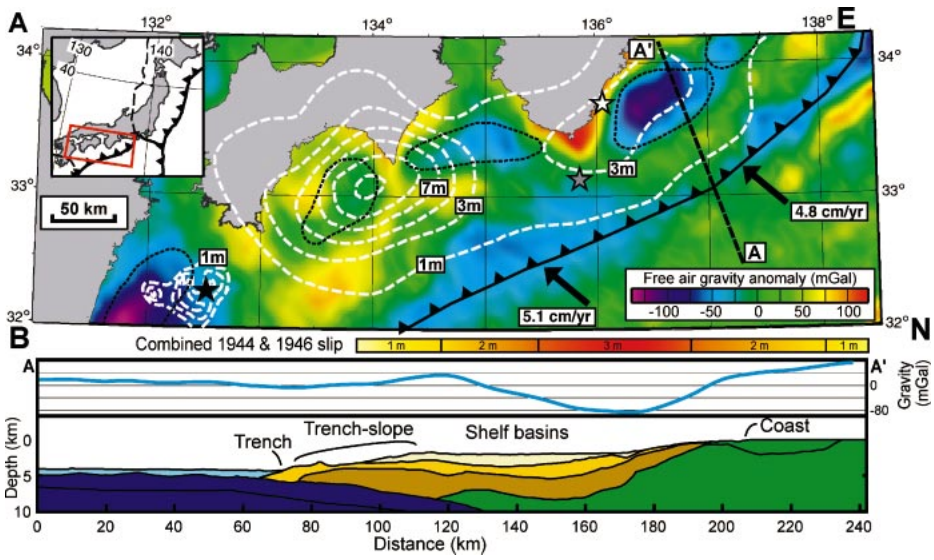

Figure 1. A: Forearc basins, dotted black lines (Sugiyama, 1994), of the Nankai subduction zone in southwest Japan are associated with free-gravity anomaly lows (color field) (Sandwell and Smith, 1997). Dashed white lines indicate seismic slip (2 m contour interval) during the 1968 M_w 7.5 earthquake (black star) (Yagi and Kikuchi, 2003) and combined 1944 M_w 8.1 (white star), and 1946 M_w 8.3 (gray star) earthquakes (Sagiya and Thatcher, 1999). B: Interpreted crustal structure (Nakanishi et al., 2002), free-air gravity anomaly, and seismic slip during 1944 M_w 8.1 and 1946 M_w 8.3 earthquakes along line A–A′. Gravity low and maximum seismic slip during 1944 and 1946 great-thrust earthquakes are associated with forearc basins. Colors in cross section correspond to the following interpreted lithologies and p-wave velocities: light blue: oceanic sediments (1.7–2.0 km/s); dark blue: oceanic crust (4.5–6.9 km/s); light yellow, orange, and brown: accreted sediments in subduction wedge (1.6–2.5 km/s, 2.0–2.9 km/s, and 3.1–4.7 km/s respectively); green, older crust (5.0–5.9 km/s). (Adapted from Wells et al., 2003.)

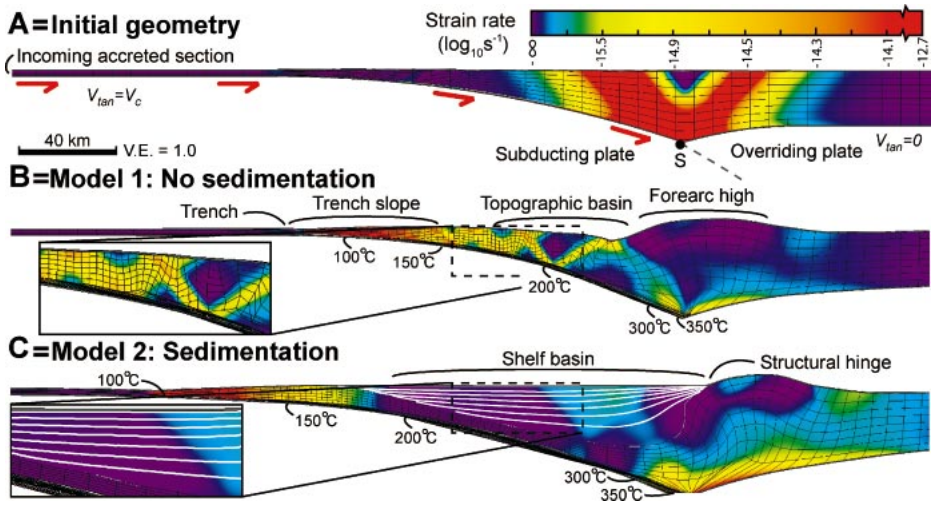

Figure 2. Numerical models for plane-strain, viscous-plastic deformation of a subduction wedge driven by basal traction and sediment accretion (see material in Data Repository [see footnote 1]). Color field shows strain rate (second invariant of strain rate tensor), and Lagrangian mesh shows integrated deformation. A: Model immediately after start of convergence representing a continental margin prior to initiation of subduction. B: Model 1 (no sedimentation) at 5 m.y. Lagrangian mesh and strain rate show active deformation throughout wedge, from trench to forearc high. Wedge deformation is primarily plastic as indicated by localizations in strain-rate field. (See Fig. DR2 and Video DR1 in Data Repository for additional details.) C: Model 2 (sedimentation) shown at 5 m.y. with parameterization identical to Model 1 except that topographic basin is filled with sediment with material properties identical to rest of the wedge. Strain rate, Lagrangian mesh, and synthetic stratigraphy of the basin (white lines) indicate little deformation of forearc basin or underlying wedge. (See Fig. DR3 and Video DR2 in Data Repository for additional details.)

an accretionary flux of ~50 km^2/m.y. (Pazzaglia and Brandon, 2001), which would mean that it would take 2.5 times longer to evolve to the same state represented by the models shown here.

Both models show the development of the main morphological features typical of forearc regions at modern convergent margins (Karig, 1974; Dickinson and Seely, 1979) (Fig. 1B). A bathymetric trench marks the surface trace of the subduction thrust, and migrates seaward as the wedge grows by accretion. Landward of the trench, the seafloor rises to a topographic and structural high that separates the lower trench slope from a shallow topographic depression or basin. Farther landward, the surface rises again, reaching a maximum at the forearc high. The active subduction thrust is located along the base of the model, extending from the trench landward. Earthquake rupture would be expected along the thrust where temperatures are low enough for seismogenic failure to occur (<~350°C) (e.g., Hyndman et al., 1995).

In Model 1 (Fig. 2B), the entire subduction wedge from the trench to the forearc high is involved in accretion-driven deformation, as shown by high strain rates and pervasive deformation of the Lagrangian mesh. The wedge shows a steady landward increase in thickness, but, for reasons discussed below, the increasing dip of the subducting plate causes a depression to form seaward of the forearc high. Temperatures in the wedge beneath the forearc high are sufficient (>350°C) to activate viscous deformation, which explains the high strain rates and strong uplift of the forearc high.

Continental margins are commonly characterized by a high sediment supply derived from the continental interior. The closed forearc depression in Model 1 is an ideal trap for these sediments. In Model 2, otherwise identical to Model 1, the depression is kept filled with sediment throughout the evolution of the subduction wedge (Fig. 2C; Fig. DR3 and Video DR2 [see footnote 1]). A comparison between the models shows that Model 2 has very low strain rates and relatively little deformation of the wedge beneath the filled basin, whereas strain rates remain large seaward of the basin and beneath the forearc high.

MODEL INTERPRETATION

The theory of critical wedges (Davis et al., 1983; Dahlen, 1984) provides a simple explanation for the development of these basins and the contrasting amounts of deformation within the wedge beneath the basins. Davis et al. (1983) were first to show that the wedge-shaped body of rock and sediment at subduction zones tends to establish a critical taper

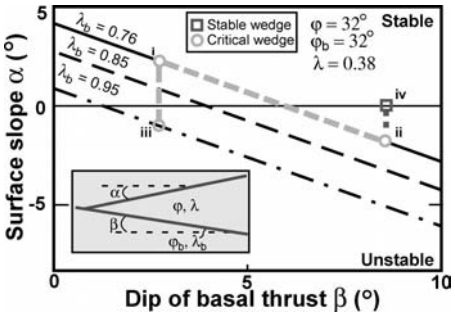

Figure 3. Relationship between surface slope α and subduction thrust dip β for a minimum-taper critical Coulomb wedge. Solution is given for 3 values of fluid pressure ratio λ_b on the subduction thrust, with other variables held constant: wedge friction φ = 32°, subduction thrust φ_b = 32°, wedge fluid pressure ratio λ = 0.38. Path i to ii represents the surface slope of a critically tapered wedge with a thrust that increases in dip landward. Landward increase in fluid pressure on the basal thrust also results in a landward decrease in surface slope (i to iii). Path ii to iv illustrates influence of sedimentation. Filling of topographic depression results in an increase of α to zero, which stabilizes the wedge beneath the basin. We refer to these basins as negative-α basins.

blunt enough that the wedge, given its intrinsic frictional strength, is able to overcome the frictional resistance to slip on the underlying subduction thrust. The accretion of new material at the front and base of the wedge causes it to increase in size. As long as the effective strength of the wedge and the subduction thrust remain constant, the wedge maintains the same critical taper. For a frictional wedge, this critical taper is a function of the basal thrust dip β, surface slope α, friction angles for the wedge φ and basal thrust φ_b, and pore fluid pressure ratio within the wedge λ and basal thrust zone λ_b (Fig. 3). This relationship defines the minimum critical taper and predicts α. Wedges with α less than critical lack the bulk strength to slide on the basal thrust and must deform internally to increase taper so that slip on the basal thrust is possible. In contrast, wedges with α greater than critical are referred to as stable given that the shear traction on the basal thrust is too small to cause deformation within the overlying wedge.

All subduction zones show a landward increase in the dip of the subduction thrust fault β due to broad flexing of the downgoing plate from its own negative buoyancy and loading by the overlying plate. The critical-taper concept indicates that as β increases, α decreases (Fig. 3). If β becomes large enough, α will become negative and the wedge will exhibit a landward-dipping surface slope. The result will be a closed depression, as shown in Model 1, where the wedge remains everywhere critical (e.g., i to ii in Fig. 3). A similar depression can also form by a landward decrease in effective strength of the subduction thrust, or a landward increase in effective strength of wedge material. Potential causes for this behavior are a landward increase in fluid pressure along the subduction thrust (i to iii in Fig. 3) or increasing lithification of wedge material.

In Model 2, the depression is filled by trapped sediments, causing the wedge to become blunter than critical by increasing the surface slope from a negative value (ii in Fig. 3) to horizontal (α = 0°) (iv in Fig. 3). Since in this model α is greater than the critical value, the wedge beneath the sedimentary basin has a stable taper. The lack of deformation beneath the basin in our numerical model reflects the fact that stable frictional wedges do not deform internally (Fig. 2C). Reflection profiles for accreting subduction wedges (e.g., Scholl et al., 1987) show that forearc basins of this type typically remain little deformed during their evolution, supporting our conclusion that the underlying wedge is stable and undeforming, not critical. We refer to these basins as negative-α basins, given that the basinal depression is formed by reversal in the surface slope above a critical wedge. This mechanism is easily distinguished from other interpretations for the formation of forearc basins, such as tectonic erosion at the base of the wedge (Wells et al., 2003) or by elastic loading during the earthquake cycle (Song and Simons, 2003).

DISCUSSION AND CONCLUSIONS

We conclude that the basins observed along the Nankai subduction zone (Fig. 1A), and similar basins along other actively accreting subduction margins (Pavlis and Bruhn, 1983; Wells et al., 2003; Song and Simons, 2003), are negative-α basins. Beneath these basins, the subduction wedge is stable and has little permanent internal deformation. In contrast, regions that lack negative-α basins are more likely to be critical and thus to have pervasive internal deformation.

An important question is why does seismic coupling appear to correlate with forearc basins (Wells et al., 2003; Song and Simons, 2003)? The slip behavior of a fault zone is thought to be related to the time- and rate-dependence of the frictional properties of the fault (Scholz, 1989; Marone, 1998a, 1998b; Scholz, 1998). In particular, Marone (1998a, 1998b) argues that fault zones become more prone to seismic slip as the rate of loading of the fault zone increases. We expect the loading rate of the subduction thrust to be greatest where the overlying wedge is stable, given that nearly all plate convergence is taken up as discrete slip on that thrust. The loading would be slower in areas where the overlying wedge is critical, given that deformation of the wedge accommodates more of the plate convergence. In addition, the stick-slip process requires an alternation between rupture and healing of the fault zone. The subduction thrust moves less frequently beneath a stable wedge, given that the upper plate of the fault zone does not deform. This situation implies long hold times, where the fault zone remains stationary. Experiments by Marone (1998a, 1998b) show that the stress drop at failure increases with longer hold time. Wibberley and Shimamoto (2005) argue that thermal pressurization is the process dominating the level of stress drop during earthquakes. This mechanism requires low permeability in the fault zone so that thermally induced pore fluid pressures can be maintained during the rupture event. The lack of deformation in a stable wedge would favor the development of low permeability above the subduction thrust. Active deformation within an overlying critical wedge would increase permeability and inhibit thermal-induced overpressures. Any or all of these processes suggest that seismic coupling should be greatest beneath stable regions of the subduction wedge.

Our models demonstrate that changes in slab dip can lead to the formation of a negative-α basin, which in turn will stabilize the subduction wedge. We note that this result can be caused by other factors. For instance, spatial variations in fluid pressure on the subduction thrust (Kastner et al., 1998) or variations in wedge strength, as occurs by lithification (Zhao et al., 1986), could cause changes in taper similar to those caused by changes in slab dip.

Wedge stability is not the only factor influencing the slip behavior of subduction zones (e.g., Kanamori, 1971; Kelleher et al., 1974; Ruff and Kanamori, 1980; Tichelaar and Ruff, 1993). Temperature plays an important role in influencing the downdip extent of the seismogenic zone on subduction thrusts (Hyndman et al., 1995). Our modeling shows that deformation mechanisms within the overlying wedge change from frictional to viscous where the subduction thrust reaches 300–350°C (Fig. 2C), which roughly coincides with the limiting temperature for seismic slip on the subduction thrust. The steeper slopes on the seaward side of the forearc high mark this transition from frictional to viscous deformation. This relationship may account for the observation of Ruff and Tichelaar (1996) that modern coastlines coincide with the downdip limit of seismic rupture at many subduction zones.

It is important to note that some subduction wedges may not be capable of reaching a negative-α taper. The wedge may be too small, the subduction thrust too strong, the dip of the thrust too shallow, or the subduction wedge too weak or too hot. In these cases, we would not expect the critical state of the subduction wedge to influence seismic coupling on the thrust.

ACKNOWLEDGMENTS

This research was supported by grants from the National Science Foundation (Willett, EAR-0208190; Brandon, EAR-0208371) and a University of Washington Peter Misch Fellowship to Fuller. The Generic Mapping Tools software of Wessel and Smith was used in making Fig. 1. We thank John Suppe and J. Casey Moore for comments on an earlier version of the paper, and to Stephan Sobolev and an anonymous reviewer for critical reviews.

REFERENCES CITED

Dahlen, F.A., 1984, Noncohesive critical Coulomb wedges: An exact solution: Journal of Geophysical Research, v. 89, p. 10,125–10,133.

Davis, D., Suppe, J., and Dahlen, F.A., 1983, Mechanics of fold-and-thrust belts and accretionary wedges: Journal of Geophysical Research, v. 88, p. 1153–1172.

Dickinson, W.R., and Seely, D.R., 1979, Structure and stratigraphy of forearc regions: American Association of Petroleum Geologists Bulletin, v. 63, p. 2–31.

Hyndman, R.D., Wang, K., and Yamano, M., 1995, Thermal constraints on the seismogenic portion of the southwestern Japan subduction thrust: Journal of Geophysical Research, v. 100, p. 15,373–15,392, doi: 10.1029/95JB00153.

Kanamori, H., 1971, Great earthquakes at island arcs and the lithosphere: Tectonophysics, v. 12, p. 187–198, doi: 10.1016/0040-1951(71)90003-5.

Kanamori, H., 1986, Rupture process of suduction-zone earthquakes: Annual Reviews of Earth and Planetary Sciences, v. 14, p. 293–322, doi: 10.1146/annurev.ea.14.050186.001453.

Karig, D.E., 1974, Evolution of arc systems in the western Pacific: Annual Reviews of Earth and Planetary Sciences, v. 2, p. 51–75, doi: 10.1146/annurev.ea.02.050174.000411.

Kastner, M., Zheng, Y., Laier, T., Jenkins, W., and Ito, T., 1998, Geochemistry of fluids and flow regime in the decollement zone at the northern Barbados Ridge: Ocean Drilling Program, Scientific results, v. 156, p. 311–319.

Kelleher, J., Savino, J., Rowlett, H., and McCann, W., 1974, Why and where great thrust earthquakes occur along island arcs: Journal of Geophysical Research, v. 79, p. 4889–4899.

Lay, T., Kanamori, H., and Ruff, L., 1982, The asperity model and the nature of large subduction zone earthquakes: Journal of Earthquake Prediction Research, v. 1, p. 3–71.

Marone, C., 1998a, The effect of loading rate on static friction and the rate of fault healing during the earthquake cycle: Nature, v. 391, p. 69–72, doi: 10.1038/34157.

Marone, C., 1998b, Laboratory-derived friction laws and their application to seismic faulting: Annual Reviews of Earth and Planetary Sciences, v. 26, p. 643–696, doi: 10.1146/annurev.earth.26.1.643.

McCaffrey, R., 1994, Global variability in subduction thrust zone forearc systems: Pure and Applied Geophysics, v. 142, p. 173–224, doi: 10.1007/BF00875971.

Nakanishi, A., Takahashi, N., Park, J.O., Miura, S., Kodaira, S., Kaneda, Y., Hirata, N., Iwasaki, T., and Nakamura, M., 2002, Crustal structure across the coseismic rupture zone of the 1944 Tonankai earthquake, the central Nankai Trough seismogenic zone: Journal of Geophysical Research, v. 107, p. 2007, doi: 10.1029/2001JB000424.

Pavlis, T.L., and Bruhn, R.L., 1983, Deep-seated flow as a mechanism for uplift of broad forearc ridges and its role in the exposure of high P/T metamorphic terranes: Tectonics, v. 2, p. 473–497.

Pazzaglia, F.J., and Brandon, M.T., 2001, A fluvial record of long-term steady state uplift and erosion across the Cascadia forearc high, western Washington State: American Journal of Science, v. 301, p. 385–431.

Ruff, L., and Kanamori, H., 1980, Seismicity and the subduction process: Physics of the Earth and Planetary Interiors, v. 23, p. 240–252, doi: 10.1016/0031-9201(80)90117-X.

Ruff, L.J., and Tichelaar, B.W., 1996, What controls the seismogenic plate interface in subduction zones? *in* Bebout, et al., eds., Subduction top to bottom., American Geophysical Union, Geophysical Monograph, Volume 96, p. 105–111.

Sagiya, T., and Thatcher, W., 1999, Coseismic slip resolution along a plate boundary megathrust: The Nankai Trough, southwest Japan: Journal of Geophysical Research, v. 104, p. 1111–1129, doi: 10.1029/98JB02644.

Sandwell, D.T., and Smith, W.H.F., 1997, Marine gravity anomaly from Geosat and ERS 1 satellite altimetry: Journal of Geophysical Research, v. 102, p. 10,039–10,054, doi: 10.1029/96JB03223.

Scholz, C.H., 1989, Mechanics of faulting: Annual Reviews of Earth and Planetary Sciences, v. 17, p. 309–334, doi: 10.1146/annurev.ea.17.050189.001521.

Scholz, C.H, 1998, Earthquakes and friction laws: Nature, v. 391, p. 37–42, doi: 10.1038/34097.

Song, T.-R.A., and Simons, M., 2003, Large trench-parallel gravity variations predict seismogenic behavior in subduction zones: Science, v. 301, p. 630–633, doi: 10.1126/science.1085557.

Sugiyama, Y., 1994, Neotectonics of Southwest Japan due to the right-oblique subduction of the Philippine Sea plate: Geofisica International, v. 33, p. 53–76.

Thatcher, W., 1990, Order and diversity in the modes of circum-Pacific earthquake recurrence: Journal of Geophysical Research, v. 95, p. 2609–2623.

Tichelaar, B.W., and Ruff, L.J., 1993, Depth of seismic coupling along subduction zones: Journal of Geophysical Research, v. 98, p. 2017–2037.

Wells, R.E., Blakely, R.J., Sugiyama, Y., Scholl, D.W., and Dinterman, P.A., 2003, Basin-centered asperities in great subduction zone earthquakes: A link between slip, subsidence and subduction erosion?: Journal of Geophysical Research, v. 108, p. 2507, doi: 10.1029/2002JB002072.

Wibberley, C.A.J., and Shimamoto, T., 2005, Earthquake slip weakening and asperities explained by thermal pressurization: Nature, v. 436, p. 689–692, doi: 10.1038/nature03901.

Willett, S.D., 1992, Dynamic and kinematic growth and change of a Coulomb wedge, *in* McClay, K.R., ed., Thrust Tectonics: London, Chapman and Hall, p. 19–31.

Willett, S.D., and Pope, D.C., 2003, Thermomechanical models of convergent orogenesis: Thermal and rheological dependence of crustal deformation, *in* Karner, G.D., et al., eds., Rheology and deformation of the lithosphere at continental margins: New York, Columbia University Press, p. 166–222.

Yagi, Y.J., and Kikuchi, M., 2003, Partitioning between seismogenic and aseismic slip as highlighted from slow slip events in Hyuga-nada, Japan: Geophysical Research Letters, v. 30, p. 1087, doi: 10.1029/2002GL015664.

Zhao, W.-L., Davis, D.M., Dahlen, F.A., and Suppe, J., 1986, Origin of convex accretionary wedges: Evidence from Barbados: Journal of Geophysical Research, v. 91, p. 10,246–10,258.

Manuscript received 9 May 2005
Revised manuscript received 26 September 2005
Manuscript accepted 8 September 2005

Printed in USA

Details for Numerical Model Used in Fuller et al.

A coupled mechanical-thermal model, used in previous studies (Willett, 1992; Willett and Pope, 2003) of collisional wedges, was modified to account for features associated with a subduction wedge, such as accretion of a relatively thin sedimentary layer and flexure of two elastic half plates. The subduction process is simulated with a hybrid kinematic-dynamic method in which the subducting slab and mantle of both plates have a prescribed motion, but the crust of the overriding plate is allowed to deformation in response to body forces and boundary velocities. The model has two domains over which solutions are obtained: a mechanical domain extending from the base of the crust to the surface (Fig. DR1a), and a thermal-kinematic domain extending from the upper asthenosphere to the surface (Fig. DR1b). Crustal deformation is calculated for a combined frictional plastic rheology and a thermally-activated power-law viscous rheology using a two-dimensional finite element method. Frictional plastic deformation is calculated using a non-linear viscosity formulism that mimics the limit condition associated with the Coulomb yield criterion. This method is capable of simulating deformation of frictional materials, such as sand and rock, and has been verified by comparison to the analytical solutions of the critical wedge theory (Willett, 1992; Willett and Pope, 2003).

Velocity boundary conditions drive deformation within the mechanical domain. The basal boundary has a specified tangential velocity, equal to the convergence velocity v_c, to the left of the point S, and zero to the right of S. The subduction thrust is simulated by a thin low-strength zone located at the base of the model to the left of the point S (Fig. DR1).

The upper surface is stress free, and its position and velocity is determined dynamically during the calculation. In Model 2 the surface is modified by sedimentation, which occurs by filling surface depressions to capacity. Basin sediment has the same physical properties as the subduction wedge and is assumed to be from a distal source. Neither model includes any erosion. We recognize that sediment can be supplied by erosion of the forearc high as it becomes subaerial; exclusion of this process does not affect the results presented here.

The lower boundary of the mechanical domain is allowed to move vertically to account for isostasy. The evolution of this boundary is determined using a calculation for flexural isostasy assuming two elastic half plates that remain in contact at the point S (Fig. 2a, Fig. DR1).

Temperature is determined within the larger, thermal-kinematic domain using a finite-element method to solve the two-dimensional, time-dependent heat transport equation including conduction, advection, and radiogenic heat production. Heat advection is calculated using the dynamically calculated velocity field from the mechanical domain and a kinematically prescribed velocity for the remaining regions. The slab velocity is prescribed at the plate convergence rate in a direction tangential to the boundary between the two plates.

Model results presented here were run with convergence velocity v_c = 50 km/Ma and an accretionary thickness h = 2.5 km, indicating an accretionary flux of 125 km^2/Ma. The nominal time in the model is inversely proportional to the accretionary flux. For example, our models (Fig. 2, DR2, DR3; Videos DR1, DR2) are directly applicable to a subduction margin with half of the accretionary flux (62.5 km^2/Ma) at twice the nominal

time shown with our results. The last step shown here with t = 6.4 Ma would correspond to a time of 12.8 Ma. This scaling argument holds as long as the thermal field in the subduction wedge remains the same, given that temperature influences the rheology. In our experience, the thermal field is only weakly dependent on accretionary flux when perturbed relative to the model conditions used here.

References

Willett, S.D., 1992, Dynamic and kinematic growth and change of a Coulomb wedge, *in* McClay, K.R., ed., Thrust Tectonics: London, Chapman and Hall, p. 19-31.

Willett, S.D., and Pope, D.C., 2003, Themo-Mechanical Models of Convergent Orogenesis: Thermal and Rheological Dependence of Crustal Deformation, *in* Karner, G.D., Taylor, B., Drisoll, N.W., and Kohlstedt, D.L., eds., Rheology and Deformation of the Lithosphere at Continental Margins: New York, Columbia University Press, p. 166-222.

Figure DR1: Boundary conditions and parameterization of the coupled thermo-mechanical model used in this study. (a) The domain of the mechanical component representing the deforming crust. The viscous rheology is characterized by a power-law exponent n, the activation energy Q, and pre-exponential A_o. The Coulomb yield criterion is characterized by the internal angle of friction φ and cohesion C. The detachment is assigned a lower friction angle φ_b, so that it is weaker than the wedge. In the paper, we define four parameters: two friction angles (φ for the wedge and φ_b for the basal thrust) and two fluid pressure parameters (λ for the wedge and λ_b for the basal thrust). The numerical model does not calculate fluid pressures, so φ and φ_b in the model are used as effective friction angles that include the influence of fluid pressure. The basal boundary has an imposed tangential velocity v_{tan}. To the left of the point S, $v_{tan} = v_c$, which is the plate convergence velocity, and to the right of S, $v_{tan} = 0$. The evolution of the lower boundary of the dynamic model is calculated assuming flexural isostasy for two elastic half plates with rigidities D_p and D_r that are kept in contact at point S. Densities are 2800 kg/m^3 for the crust, 3300 kg/m^3 for the mantle, and 1030 kg/m^3 for water. (b) The domain of the thermal model, extending from the surface to the asthenosphere. The velocity field v, used to calculate heat advection, is taken from the velocity solution in the mechanical domain (green) described in (a), and the kinematic velocity for the subducting lithosphere. The slab velocity is set at v_c in the direction tangent to the surface of the subducting lithosphere. The slab geometry is initially prescribed, but subsequently allowed to evolve due to the flexural isostatic response of the lithosphere to the changes in crustal load as described above. Radiogenic heat production H is non-zero and uniform in the crust and zero elsewhere. The thermal conductivity k of the upper asthenosphere is set artificially high to simulate the approximately isothermal condition associated with a convecting mantle. Specific heat capacity c_p is uniform throughout the model domain.

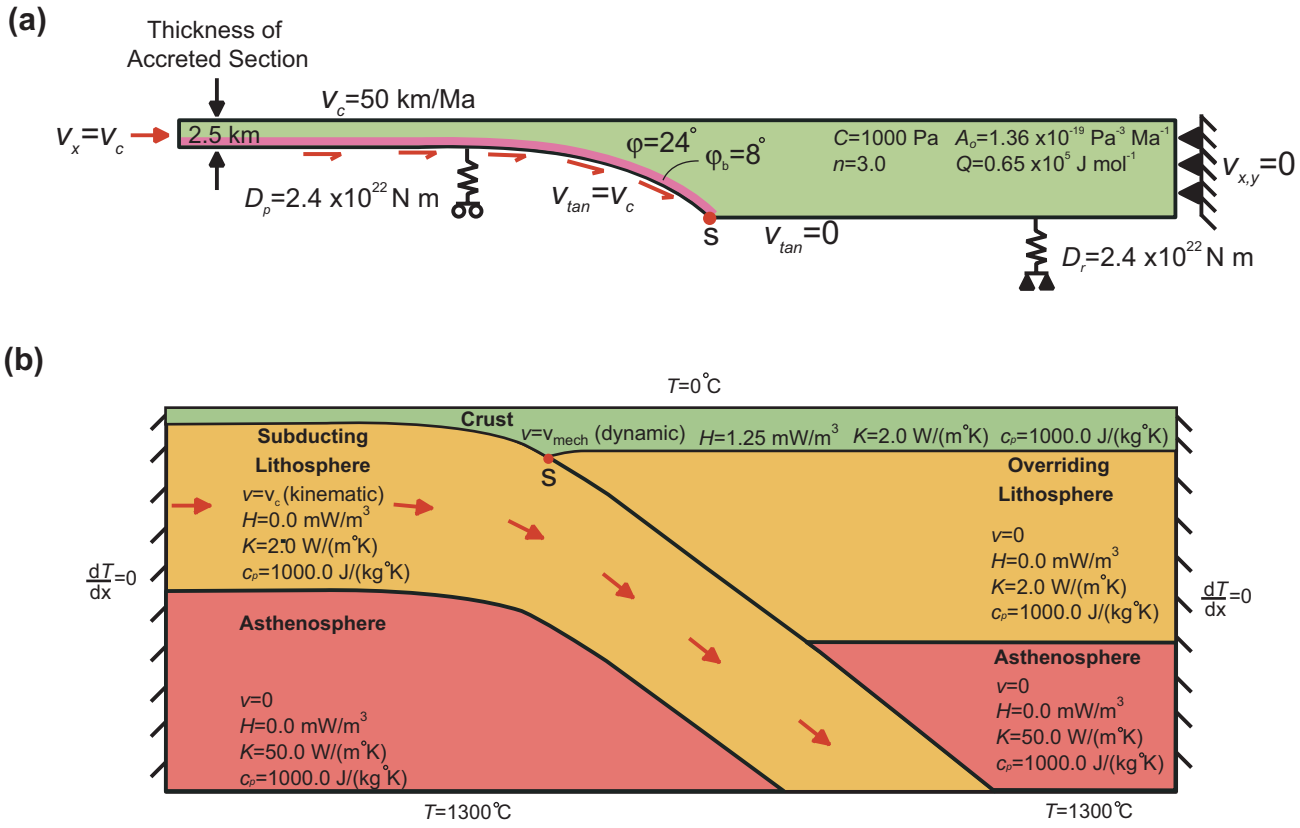

Fuller et al., 2005. Fig. DR1

Figure DR2 and Video DR1: Evolution of Model 1, with no sedimentation, shown in Fig. 2b. A nominal time *t* is shown in Ma and is calculated for a convergence velocity of 50 km/Ma and a 2.5 km thickness of accreted sediment. The colors indicate strain rate (second invariant of the strain rate tensor). The Lagrangian mesh is a passive feature that shows the integrated motion and deformation in the wedge. Note the persistent deformation from the trench to the landward side of the model, as shown by the strain rate and the Lagrangian mesh. Also note the seaward migration of the trench, growth of the subduction wedge, and uplift of the forearc high, as described in the text. The model has no vertical exaggeration.

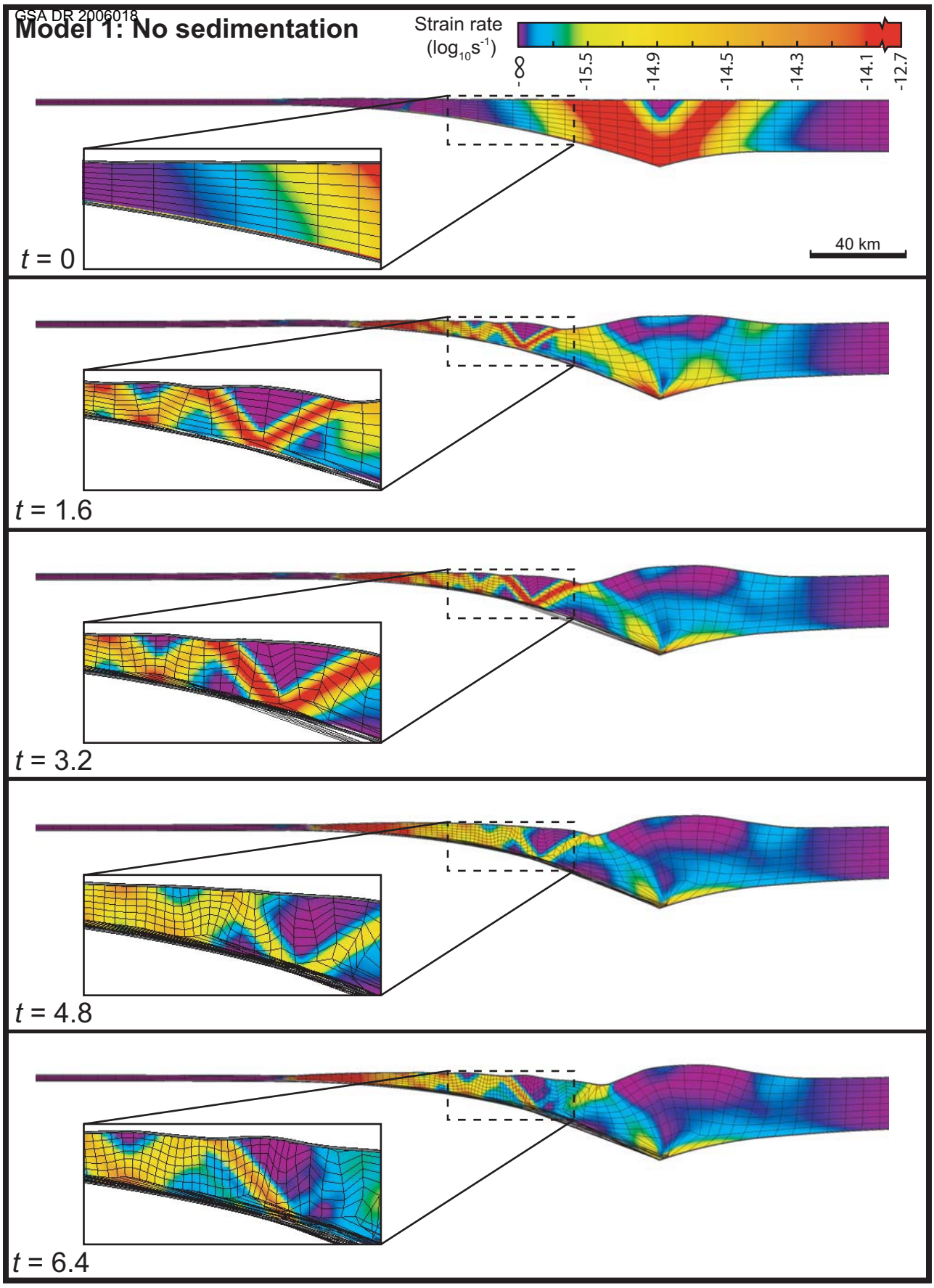

Fuller et al., 2005. Fig. DR2

Figure DR3 and Video DR2: Evolution of Model 2, including sedimentation, shown in Fig. 2C. The nominal time, *t*, is given in Ma, using the same convergence velocity and accretionary thickness as in Fig. DR2 and Video DR1. The synthetic stratigraphy (indicated by white lines) shows the growth of the forearc basin. Strain rates are high seaward of the basin, but very low beneath the basin. The model has no vertical exaggeration.

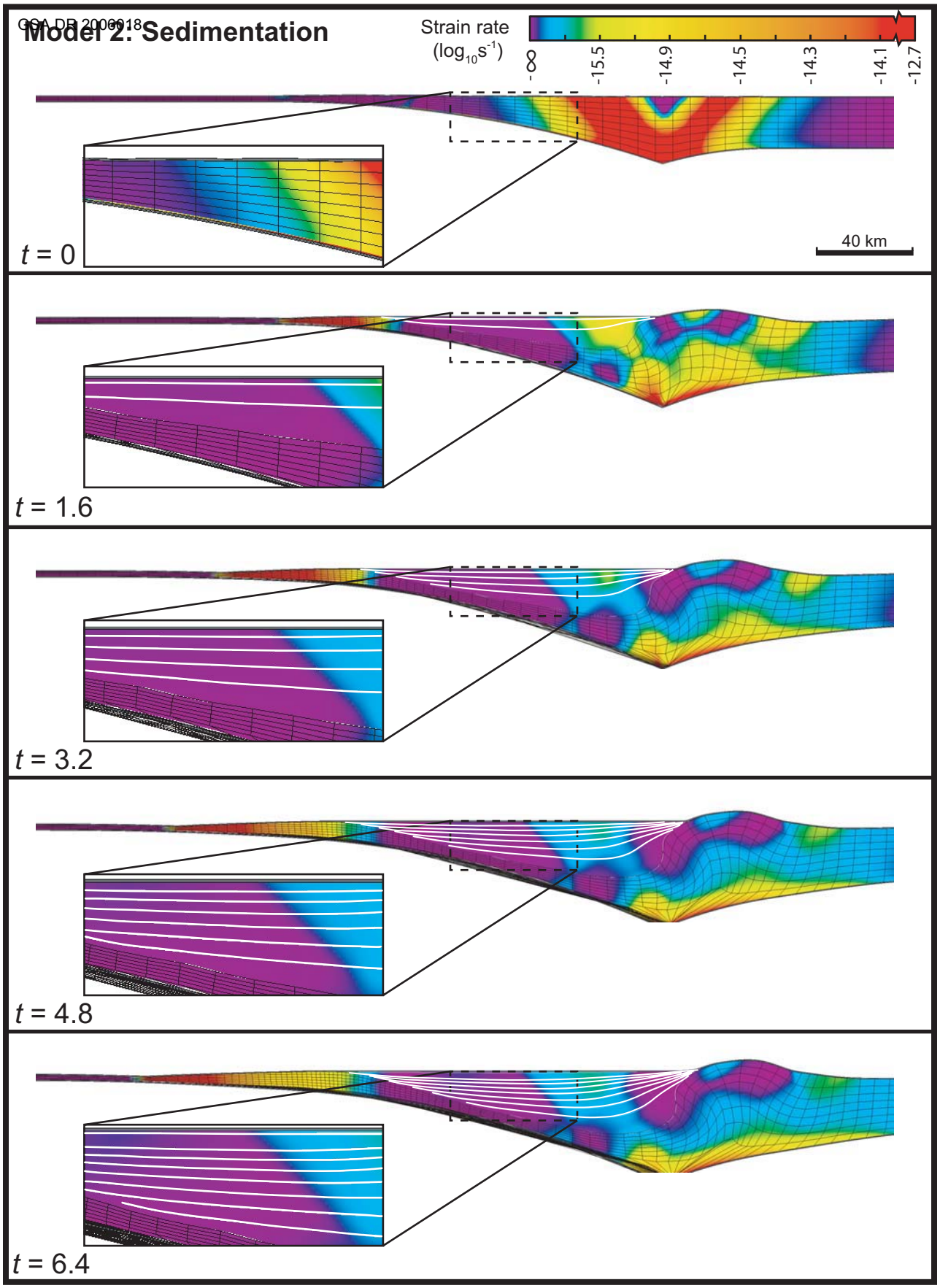

Fuller et al., 2005. Fig. DR3